Acta Technica *62* (2017), No. 5B, 1013–1024

Simulation and analysis on walking features of walking robot on the transmission line

Huang Chen[2], Xiao Ai-ping[2,3], Qian Hua[2]

Abstract. Based on current research of Walking Robot on high-voltage line, this paper presented a new type of Walking Robot, which could achieve stable and reliable online travel through ordered clamping and releasing of three clamping jaws together with cooperative working of two obstacle-surmounting plates. Considering the flexibility of high-voltage line, the online travel of robot was classified into uphill and downhill in the walking process, and the effects of lifting movement caused by the middle jaw on the whole movement were investigated in detail. On this basis, dynamic equations of the uphill movement were established and ADAMS was applied to analyze and simulate the dynamics of the robot. It was found that the simulation results agreed well with the theoretical computation results, thus providing some important bases for the development of motion control system.

Key words. Walking Robot, Middle-gripper, Lifting and Lowering Movements, ADAMS.

1. Introduction

Walking robots on the transmission line are mainly used to inspect and clean ice on the line, so that there are high requirements for their flexibility and versatility. Generally, walking robots can realize inspection of the high-voltage line after installed with inspection equipment and complete de-icing work of the high-voltage line after installed with de-icing equipment. In order to improve the efficiency of de-icing and inspection, and meanwhile protect workers and reduce losses, anew, economical, safe and effective walking robot that can replace or partially replace workers should be developed.[1]

At present, the studies of inspection and de-icing walking robot on the high-voltage line are still in the laboratory stage, and no practical products have been reported yet. Among these studies, some typical robot prototypes are worthy of

[1]Acknowledgment - This paper is supported by the Fundamental Research Funds for the Central Universities with project number:YX2011-7.

[2]Workshop 1 - School of Technology, Beijing Forestry University, Box 8, Beijing 100083, China

[3]Corresponding author: Xiao Ai-ping ;email:huangchen620@163.com

careful attention. For example, the inspection robot produced by Sato Company in Japan[2] and the HQ LineROVer developed by IREQ-Quebec Research Institute on Electricity in Canada[3],which can work on the line between two towers; the TRC inspection robot developed by the USA [4]and the two-arm and three-arm inspection robot developed by the Institute of Automation of the Chinese Academy of Sciences, which can surmount obstacles [5].However, it should be noticed that the control of three-arm inspection robot is complex, and that the stability of the two-arm inspection robot is not very good. Moreover, the adjustment on the center of gravity is very difficult when the two-arm or three-arm inspection robot surmounts obstacles.[6]

Because of the flexibility of high-voltage line,[7] there are attitude changes of uphill and downhill when walking robot walks online, which leads to the poor stability of inspection and de-icing robot. [8]In view of this, a new walking robot with jaws and obstacle disk is designed, which cannot only walk normally and stably online, but also facilitates the installment of de-icing and inspection equipments, thus achieving a multi-purpose function. This paper focuses on stress analysis and kinetic modeling of two attitudes in the uphill process online, and then carries out the dynamic simulation by ADAMS to further demonstrate the beneficial effects of lowering the middle jaw on the whole movement. Finally, the feasibility of the design is verified by means of experiments.

2. Structural design and working principle of the robot

2.1. Structural Design

The overall structural design of the walking robot on high-voltage line can be seen in Figure 1, which includes the jaw mechanism, the walking mechanism, the obstacle-surmounting mechanism. Its overall size is 900mm * 237mm * 317mm, the effective stroke is 437mm, the weight is 25kg, and the running speed is 0.5m/min.

2.2. Working Principle

The robot has two operating modes: normal mode and obstacle-surmounting mode. In normal operating mode, two obstacle-surmounting plates remain stationary on the high-voltage line in order to play a supportive and guiding role; the front and rear jaws grip the transmission line and the middle jaw opens up; the feed motor rotates in forward direction so that the middle jaw moves forward near the front jaw. When the distance sensor on the middle jaw detects that the distance between the front jaw and the middle jaw is the setting distance, the feed motor stops rotating. Then, the middle jaw grips the transmission line, and the front and rear jaws open up to release the transmission line. Afterwards, the feed motor starts to rotate in reverse direction, thus making the machine go forward. In obstacle-surmounting mode, the front and rear jaws grip the high-voltage line, and the middle jaw opens up and moves forward to the fixed position of the front obstacle-surmounting plate. Then, it grips the transmission line, and the front and rear jaws open up. The lifting

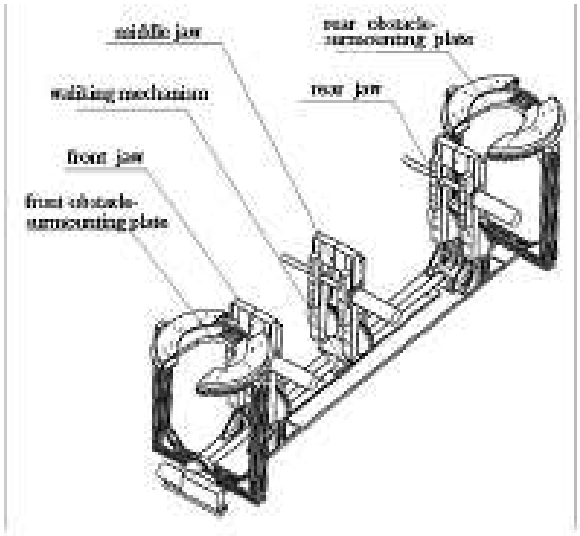

Fig. 1. The overall structural design of walking robot

mechanism of the middle jaw moves downward to reduce the distance between the cramping and the de-icing machine, and meanwhile the obstacle-surmounting plate breaks away from the transmission line completely to guarantee a certain distance between the obstacle-surmounting plate and the transmission line (the safe distance is defined as not touching the transmission line when the obstacle-surmounting plate is rotating).Driven by the motor through the gears, the obstacle-surmounting plate rotates 180 degrees around the obstacle. After completely surmounting the obstacle, the lifting mechanism of the middle jaw moves forward to make the front obstacle-surmounting plate contact with the transmission line again, and thus the whole machine moves forward. After the front plate moves forward by a certain distance (the safe distance should meet the requirement that the distance between the rotation center of the obstacle-surmounting plate and the obstacle is greater than the obstacle's radius), the middle jaw moves forward again and reduces the distance between the cramping and the de-icing machine. At the same time, the obstacle-surmounting plate breaks away from the transmission line completely to guarantee a certain distance between the obstacle-surmounting plate and the transmission line (the safe distance is defined as not touching the transmission line when the obstacle-surmounting plate is rotating).Then, the obstacle-surmounting plate rotates 180 degrees in reverse direction in order to restore its original state, thus making the obstacle-surmounting plate traverse the obstacles stably. Figure 2 presents the physical prototype of the robot.

Fig. 2. Physical prototype of the robot

3. Mathematical model

Because of the flexibility of high-voltage line, there are bound to attitude changes of uphill and downhill when the walking robot is online due to the effect of its own gravity. For both attitudes, the whole machine operates through the middle jaw gripping the high-voltage line. In this study, only the attitude of uphill is analyzed and modeled, and the attitude of downhill can be analyzed and modeled analogously. Considering the effect of elevating operation of the middle jaw on the dynamic characteristics of the robot in normal movement, we analyze the attitude of uphill under two conditions, i.e., three jaws with the same height and the middle jaw a little lower than the others. According to the movement principle, under both conditions, the middle jaw grips the transmission line without moving out of the position, which means its relative position in the direction along the same transmission line is not changed. Assume that the friction between the gripper and the line isf_C, the front and rear obstacle-surmounting plates move forward by the driving force between the middle jaw and the prismatic joint of the base, and that the friction between the wheels of the front and rear disk and the line is rolling friction.

3.1. Three Jaws with the Same Height

The robot is simplified into the following models shown in Figure 3. Here, only the situation that the middle jaw grips the transmission line and the front and rear jaws open up is analyzed. As long as the middle jaw grips the transmission line, the front and rear jaws are bound to provide sufficient clamping force to ensure that the machine does not slip no matter in uphill or downhill process. In this model, the front and rear obstacle-surmounting plates are simplified as two wheels with a radius of R, the front and rear jaws and the base are regarded as one whole, the centroids of all bars are at their center positions, and the middle jaw has the same length with the front and rear obstacle-surmounting disks, namely the angle between the horizon and the whole machine isδ.The accelerations of starting and stopping are both set as a,

$O_AA = O_BB = O_CC = D^*D = h$, and $O_AO_B = AB = d$

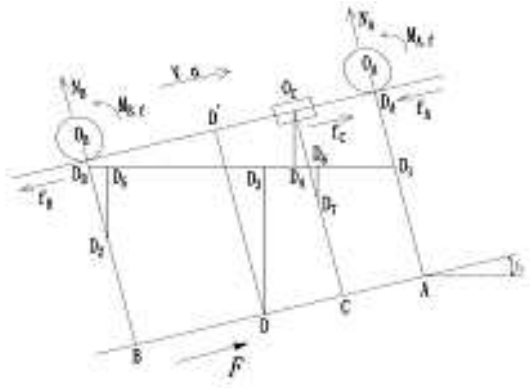

Fig. 3. Uphill attitude when the three jaws have the same height

The mechanical equilibrium equations can be expressed as follows:

$f_C - f_A - f_B - m_1 g \sin\delta - m_2 a = 0$

$N_A + N_B - m_1 g \cos\delta = 0$

$-M_{A,f} - M_{B,f} + m_A g D_1 D_4 + m_C g D_6 D_4$

$-m_B g D_5 D_4 - m_{AB} g D_3 D_4 + N_B O_B O_C - N_A O_A O_C$

$-(m_A + m_B) a O_C D_7 - m_{AB} a D D^* = 0$

$-M_{A,f} + f_A R = 0$

$M_{A,f} = \delta_A N_A$

$-M_{B,f} + f_B R = 0$

$M_{B,f} = \delta_B N_B$

$M_{A,f}, M_{B,f}$——Rolling friction couple between the front obstacle-surmounting plate, the rear obstacle-surmounting plate and the transmission line;

f_A, f_B, f_C——Dynamic friction between the front obstacle-surmounting plate, the rear obstacle-surmounting plate, the middle jaw and the transmission line;

δ_A, δ_B——Coefficient of rolling friction couple between thefront obstacle-surmounting plate, the rear obstacle-surmounting plate and the transmission line.

Substituting the known conditions into the above equations, it can be obtained:

$f_C \geq m_1 g \sin\delta + m_2 a + m_3 g \delta_A \cos\delta / R - F$

in which,

$$m_1 = m_A + m_B + m_C + m_{AB} m_2 = m_A + m_B + m_{AB}$$
$$m_3 = m_A + m_B + m_C + 2 m_{AB} m_4 = m_A + m_B + 2 m_{AB}$$

3.2. Middle Jaw a Little Lower than the Others

Through above analysis on the attitude, the friction $f_C$between the middle jaw and the transmission line in uphill process can be obtained, and further the torque of the jaw's driving motor can be figured out. The frictional force $f_C$can be provided not only by the positive pressure??f_{C1}??from the jaw clamping to the transmission line, but also by part of the machine weight ??f_{C2}??. Hence, we can reduce the value off_{C1}, and thereby reduce the required force of the clamping jaws gripping

the transmission line. As a result, the torque of the selected driving motor can be properly reduced, which can ensure that clamping jaw grips the transmission line better, thus making the machine walk online stably. In this case, the length of the middle jaw is variable, namely$O_CC = x$. Figure 4shows the movement attitude of the robot in the uphill when the height of the middle jaw is lowered.

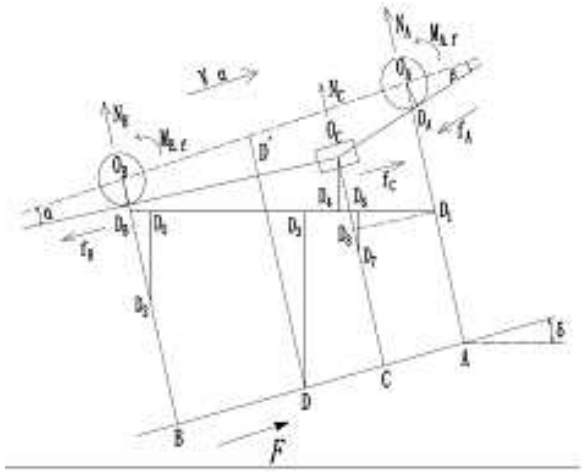

Fig. 4. Uphill movement attitude of robot when the height of the middle jaw is lowered

Mechanical equilibrium equations are as follows:

$$f_C + f_C^* - f_A\cos\beta - f_B\cos\alpha - N_A\sin\beta$$
$$+N_B\sin\alpha - m_1 g\sin\delta - m_2 a = 0$$
$$N_C + N_A\cos\beta + N_B\cos\alpha - m_1 g\cos\delta$$
$$-f_A\sin\beta - f_B\sin\alpha = 0$$
$$M_{A,f} + M_{B,f} + m_A g D_1 D_4 + m_C g D_6 D_4$$
$$-m_B g D_5 D_4 - m_{AB} g D_3 D_4 + N_B D_B O_C - N_A D_A O_C$$
$$+(m_A + m_B) a O_C D_8 + m_{AB} a O_C C = 0$$
$$M_{A,f} - f_A R = 0$$
$$M_{A,f} = \delta_A N_A$$
$$M_{B,f} - f_B R = 0$$
$$M_{B,f} = \delta_B N_B$$
$$h - x = (d - d_{AC})\tan\alpha + R/\cos\alpha$$
$$h - x = d_{AC}\tan\beta + R/\cos\beta$$
$$f_C^* = uN_C$$

In which,

f_C——The friction caused by the clamping force of the middle jaw on the high-voltage line;

f_C^*——The friction caused by the component force of the clamping force of the middle jaw on the high-voltage line in the direction vertical to the travelling direction of the machine;

α——The angle between the high-voltage line$O_CD_B$and the machine AB after

the middle jaw is shortened;

β——The angle between the high-voltage line$O_C D_A$ and the machine AB after the middle jaw is shortened;

x——The height of the middle jawOO_C;

d_{AC}——The distance between the middle jaw and the front jaw along the direction of the machine, namely the distance AC;

u——The dynamic friction coefficient between the jaw and the high-voltage line.

From the above equations, combined with the geometric features, it can be obtained:

$$f_C = m_1 g \sin\delta + m_2 a + u m_1 g \cos\delta +$$
$$(1 + uR/\delta_A) f_A \cos\beta + (1 + uR/\delta_A) f_B \cos\alpha$$
$$-(R/\delta_A - u) f_A \sin\beta - (R/\delta_B + u) f_B \sin\alpha$$
$$-F$$

ince the length of the middle jaw and its position on the machine are variable, $\alpha$and$\beta$are also variable, which causes the change of the clamping force that the middle jaw acts on the transmission line, thus affecting the motion characteristics of the machine.

3.3. Comparison of $f_c$in the Two Attitudes

In order to get f_C of the two attitudes intuitively, some simplification can be made as follows. Generally, in actual operation, the acceleration is very small, so that the generated inertial force to the machine can be negligible, i.e.,$(m_A + m_B + m_{AB})a \approx 0$in Eqs. (8) and (19).Assume the two attitudes are under the same external condition (not taking the wind into account),that is, $\delta$is a constant (here,δ=20).Besides,$m_A = m_B = m_C = 6.5kg, m_{AB} = 8.5kg, h = 0.35m$,

$$d = 0.42m, R = 0.015m, u = 0.2, \delta_A = 0.003m.$$

Thus, through Mat lab, the dependency of$f_C$on$d_{AC}$for different x can be obtained, as shown in Figure5.

If the whole machine is only driven by the friction produced by the clamping force of the jaw, the required motor torque of the jaw maybe very large, and meanwhile the jaw cannot grip the high-voltage line firmly. In view of this, the robot's weight can be used to produce some part of frictional force. Combined with the clamping force, the jaw can grip the transmission line firmly, thus ensuring the stable movement of the robot.

4. Establishment of adams dynamic model and simulation analysis

To further verify the reliability of our design, Solid works is used to establish3D model of the robot, and then the 3D model is imported into ADAMS2012, as shown in Figure6. Considering the flexibility of high-voltage line, modal analysis and modeling of the high-voltage line are conducted in the simulation. Using the flexible

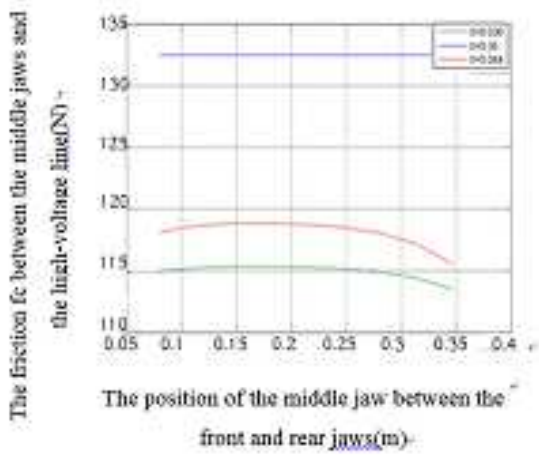

Fig. 5. $f_c$variation with d_{AC}

modeling module of ADAMS, the high-voltage line is directly transformed into rigid flexible body, which is more suitable for the actual situation. In this case, the top 25 order modal frequencies are selected. The span of the optional wire is 500m, the diameter is 9mm, the density is$3.743 \times 10^3 kg/mm^3$, the elastic modulus is$76000 N/mm^2$,and the tensions at both ends are 10000N.

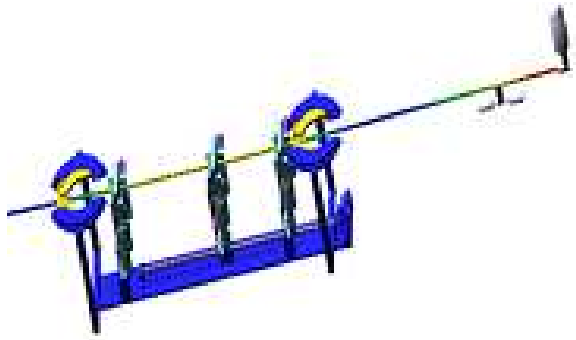

Fig. 6. The three-dimensional model and the operating environment of the robot

Here, the dynamic simulation in both cases, namely the three jaws with the same height and the middle jaw lower than the others, is carried out to obtain the variation of friction force produced by the middle jaw's clamping force with time, as shown in Figures 8 and 9.As can be seen, the curves in the figures fluctuate between 1.0 $\sim$ 1.5s, and approach to a certain value between 1.5$\sim$3s. This can be attributed to the flexibility of the line, which causes the complexity of the dynamics and kinematics of the robot. When the robot is working online, the vibration and deformation of the line may result in the difficulty of surmounting the obstacles and even serious accidents, which should be paid enough attention to. The friction force

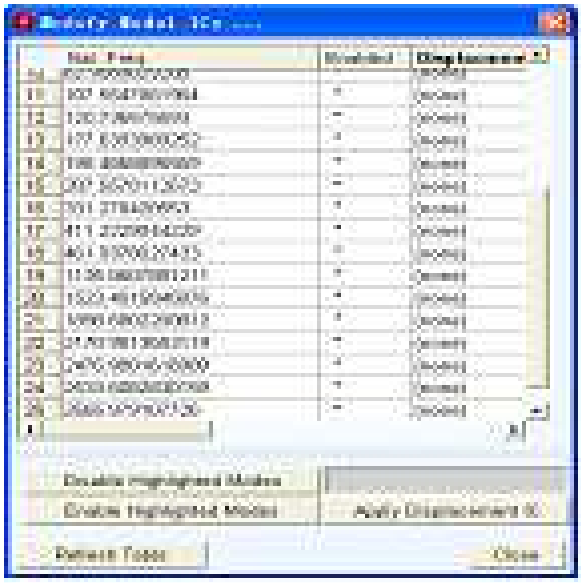

Fig. 7. Modal frequencies of the wire

in Figure9 is significantly larger than that in Figure8, which means that the friction force between the middle jaw and the high-voltage line when the middle jaw is lower than the others is larger than that when the three jaws are in the same height. That is to say, when the middle jaw is lower than the others, the clamp is more reliable, and the robot can walk on the line more stably in this situation.

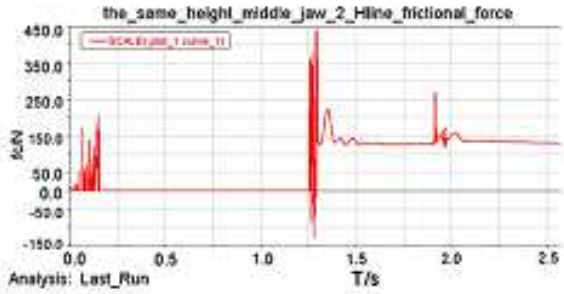

Fig. 8. The variation of friction force between the middle jaw and the high-voltage line when the three jaws are in the same height

5. Conclusion

This paper describes the structural characteristics and the working principle of the walking robot on the transmission line, and carries out dynamic modeling for its uphill process. Through calculation and analysis on two uphill attitudes, it can

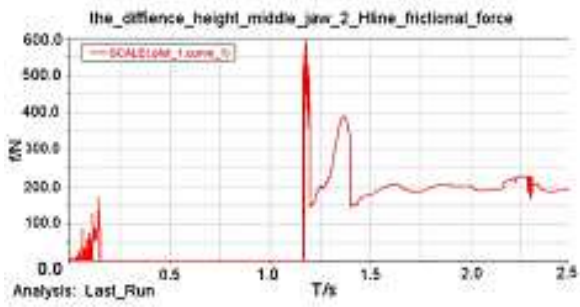

Fig. 9. The variation of friction force between the middle jaw and the high-voltage line when the middle jaw is lower (12mm) than the others

be concluded that the lifting movement of the middle jaw has a great influence on the reliability of the robot online. To take full advantage of the flexibility of high-voltage line, ADAMS is used to carry out dynamic simulation, and it is found that the friction force between the middle jaw and the transmission line when the middle jaw is lower than the others is larger than that when the three jaws are in the same height, which means that the machine can operate more stably in actual operating process. In the end, through the comparison of the two uphill attitudes, the effectiveness of the proposed theory and simulation analysis is further validated, thus confirming the reliability and feasibility of our design.

References

[1] Y. C. Zhang, Z. Z. Liang, M. Tan: *Mobile robot for overhead powerline inspection-a review.* Robot *26* (2004), 467–472.

[2] G. Paula: *Robotics:growing maintenance option for utilities.* Electrical. World *203* (1989), 65–72.

[3] X. L. Zhu, H. G. Wang: *Analysis drive dynamic performance and position-pose of autonomous robot for transmission line inspection.* Chinese journal of mechanical engineering *42* (2006), 143–150.

[4] R. P. Singh, S. K. Jain: *Free asymmetric transverse vibration of parabolically varying thickness polar orthotropic annular plate with flexible edge conditions.* Tamkang Journal of Science and Engineering *7* (2004), No. 1, 41–52.

[5] J. Y. Park, B. H. Cho, S. H. Byun, J. K. Lee: *Development of cleaning robot system for live-line suspension insulator strings.* Int. J.control autom. syst *7* (2009), No. 2, 211–220.

[6] M. Buhringer, J. Berchtold, M. Buchel: *Cable-crawler robot for the inspection of high-voltage power lines that can passively roll over mast tops.* Industrial robot: An international journal *37* (2010) 256–262.

[7] B. Franz: *Analytical techniques for retrieval of atmospheric composition with the quadrupole mass spectrometer of the Sample analysis at Mars instrument suite on Mars science laboratory.* Planetary and Space Science *96* (2014), 99–113.

[8] P. Williams: *Dynamics of a cable with an attached sliding mass.* Anziam *47* (2006), No. 1, 86–100.

[9] P. Boscariol, A. Gasparetto, V. Zanotto: *Active position and vibration control*

of a flexible links mechanism using model-based predictive control. J Dyn Syst Meas Control *132* (2010), No. 1, 506–514.

Received November 16, 2017